In situ DRIFTS study of the selective reduction of NO$_x$ with alcohols over Ag/Al$_2$O$_3$ catalyst: Role of surface enolic species

Qiang Wu, Hong He [*], Yunbo Yu

State Key Laboratory of Environmental Chemistry and Ecotoxicology, Research Center for Eco-Environmental Sciences, Chinese Academy of Sciences, Beijing 100085, China

Abstract

In situ diffuse reflectance infrared Fourier transform spectroscopy (DRIFTS) was used to clarify the formation and reactivity of enolic species and its role in the formation of the isocyanate species (–NCO) during the selective catalytic reduction of NO$_x$ (SCR of NO$_x$) by alcohols (CH$_3$OH, C$_2$H$_5$OH and isopropyl alcohol (IPA)) over Ag/Al$_2$O$_3$ catalyst. The enolic species, which was derived from the partial oxidation of C$_2$H$_5$OH and IPA in the presence of O$_2$ over Ag/Al$_2$O$_3$, had a high reactivity with NO + O$_2$, resulting in a high surface concentration of –NCO species and high efficiency of NO$_x$ reduction when using C$_2$H$_5$OH or IPA as reductants. In contrast, CH$_3$OH was much less effective for the SCR of NO$_x$. The order of the facility for the formation of enolic species and –NCO species was in good agreement with the order of the activities in the SCR of NO$_x$ process (C$_2$H$_5$OH > IPA > CH$_3$OH) in the moderate temperature range of 523–623 K.
© 2005 Elsevier B.V. All rights reserved.

Keywords: In situ DRIFTS; Ag/Al$_2$O$_3$; Selective catalytic reduction; Enolic species; Isocyanate species (–NCO)

1. Introduction

The SCR of NO$_x$ in the presence of excess O$_2$ can be applied to the removal of gaseous pollutants from diesel and lean-burn engines. In recent studies [1–10], alumina-supported silver catalysts (denoted as Ag/Al$_2$O$_3$), which are relatively durable and inexpensive, have been considered to be a candidate for practical use. In particular, C$_2$H$_5$OH is extremely effective for the SCR of NO$_x$ over Ag/Al$_2$O$_3$ even in the presence of water and SO$_2$ [1,4,5].

So far, several reaction mechanisms for NO$_x$ reduction including the intermediates (such as NO$_3^-$, CH$_3$COO$^-$, R–NO$_2$, –CN and –NCO species, etc.) have been proposed [4–7,11–18]. Among these mechanisms, –NCO species has often been proposed as a crucial intermediate. Our previous studies as well as other research works have also proved that the formation of –NCO species and its effective reaction with NO or NO + O$_2$ are key steps in the SCR reaction [4,5,11,15,17]. We recently have proposed a novel mechanism of the SCR of NO$_x$ by C$_2$H$_5$OH [19], where the surface enolic species related with the high surface concentration of –NCO and the high efficiency of NO$_x$ reduction by C$_2$H$_5$OH. However, other alcohols (such as IPA and CH$_3$OH, etc.) have not been proved to follow the same mechanism during the SCR of NO$_x$.

In this paper, we use in situ DRIFTS method to study the behavior of surface species on Ag/Al$_2$O$_3$ during the SCR of NO$_x$ using C$_2$H$_5$OH, IPA and CH$_3$OH as reductants. Particular attention is given to the surface enolic species, which formed from the partial oxidation of alcohols during the SCR of NO$_x$. The results could provide new insights into the mechanisms for the SCR of NO$_x$ by alcohols.

2. Experimental

2.1. Catalyst preparation

Ag/Al$_2$O$_3$ (5 wt.%) catalyst was prepared by an impregnation method as following: Al$_2$O$_3$ powder (200 m^2/g) was

---

* Corresponding author. Tel.: +86 10 62849123; fax: +86 10 62849123.
  E-mail address: honghe@mail.rcees.ac.cn (H. He).

dissolved in an appropriate amount of silver nitrate aqueous solution. The sample was dried at 393 K for 3 h and calcined at 873 K for 3 h in air.

2.2. Activity measurements

The catalytic activity was measured in a fixed-bed reactor by passing a gaseous mixture of NO (800 ppm), reductant (C_2H_5OH 1565 ppm or IPA 1200 ppm or CH_3OH 2250 ppm) O_2 (10%) in N_2 balance at a total flow rate of 2000 mL/min. $W/F = 0.018$ g s cm^{-3} (GHSV $\sim 50,000$ h^{-1}). NO_x conversion was analyzed on-line by a chemiluminescence NO/NO_2/NO_x analyzer (42C-hl, Thermo Environmental). An aqueous C_2H_5OH (or IPA or CH_3OH) solution was supplied with a micropump into the gas stream and vaporized by a coiled heater at the inlet of the reactor. Analysis of the gas products was carried out using a NEXUS 670-FTIR spectrophotometer fitted with a gas cell of volume 2 dm^3 (all spectra were measured with a resolution of 1 cm^{-1} and with an accumulation of 32 scans) and gas chromatography (Agilent 6890N GC) coupled to a mass spectrometer (Agilent 5973N MS) with a column-containing HP-PLOT Q (Agilent 30 m × 0.320 mm).

2.3. In situ DRIFTS procedure

In situ DRIFTS spectra were recorded on a NEXUS 670-FTIR equipped with a smart collector and a MCT/A detector cooled by liquid N_2. The catalyst was finely ground and placed in a ceramic crucible. Prior to each experiment, the catalyst was firstly heated in a flow of 10 vol% $O_2 + N_2$ for 60 min at 573 and 873 K, respectively, then cooled to the desired temperature and a spectrum of the catalyst in the flow of $N_2 + O_2$ served as the background was recorded. All gas mixtures were fed at a flow rate of 300 mL/min. All spectra were measured with a resolution of 4 cm^{-1} and with an accumulation of 100 scans.

3. Results and discussion

3.1. Reaction activity of various alcohols for the SCR of NO_x over Ag/Al_2O_3 catalyst

Fig. 1 shows the conversion of NO_x over Ag/Al_2O_3 catalyst for the various reaction systems (NO–O_2-reductant). When using C_2H_5OH as a reductant, the maximal conversion of NO_x was up to 99.7% with a very broad active temperature window (597–747 K). In the case of IPA, it is worthwhile to note that the NO_x conversion was nearly the same as that of C_2H_5OH within the temperature range of 623–773 K. In contrast, there was a relatively lower NO_x conversion by CH_3OH in the temperature range of (547–691 K) and the highest conversion of NO_x was only 21.9%. These results indicate that the NO_x conversion is strongly influenced by the kinds of alcohols and the order of the
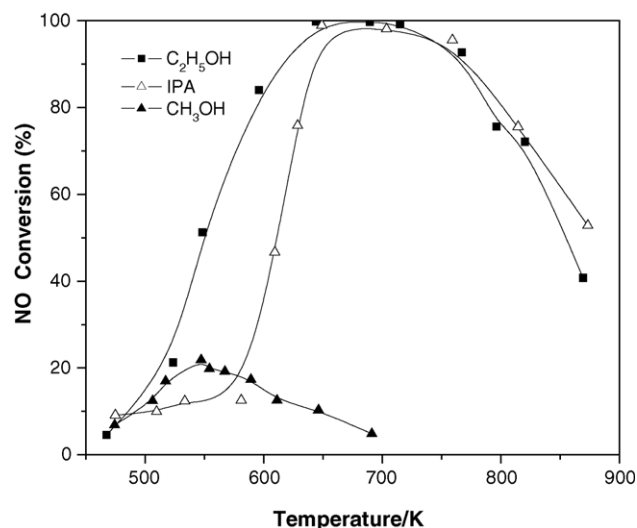

Fig. 1. Catalytic activity for NO_x reduction with different alcohols over Ag/Al_2O_3 catalyst at various temperatures. Conditions: NO 800 ppm; CH_3OH 2250 ppm or C_2H_5OH 1565 ppm or IPA 1200 ppm; O_2 10% in N_2 balance at total flow rate 2000 mL/min. $W/F = 0.018$ g s cm^{-3} (GHSV $\sim 50,000$ h^{-1}).

effective reactivity is $C_2H_5OH > IPA > CH_3OH$ in the moderate temperature range of 523–623 K.

The main products of the SCR of NO_x over Ag/Al_2O_3 catalyst are N_2 and CO_2. The diversity of by-products using different alcohols as reductants only could be seen at low temperatures, so we measure the by-product distributions at 473 K. GC–MS alone would not permit us to distinguish CO_2 from N_2O, N_2 from CO; on the other hand, N_2 is not IR active, and hence could not be detected. As a result, both the two analysis systems are used in our experiments. From FTIR gas spectra, we detected small amount of N_2O (<30 ppm) and traces of HCN and NH_3. GC–MS analysis was used to detect other nitrogen-containing species, which were not detectable by FTIR. In the reduction of NO_x with C_2H_5OH (Fig. 2A), mainly N_2 and CO_2 were produced and the reduction was accompanied by side reactions leading to the formation of acetaldehyde (CH_3CHO, 200 ppm) along with 120 ppm unreacted C_2H_5OH and small amount of nitrogen-containing compounds such as N_2O and CH_3NO_2. During the reduction of NO_x by IPA, acetone (CH_3COCH_3) was the main side product, together with other minor by-products such as C_2H_5OH, CH_3CHO, N_2O and CH_3NO_2. Traces of HCN and C_3H_6 were also present (Fig. 2B). As for CH_3OH (Fig. 2C), the main products were CO_2 and N_2, accompanied by small amount of unreacted CH_3OH. No by-products could be detected at 473 K and higher temperatures.

3.2. In situ DRIFTS study of the SCR of NO_x by different alcohols over Ag/Al_2O_3 catalyst

The difference of these three alcohols for the SCR of NO_x over the Ag/Al_2O_3 was investigated by DRIFTS method. Fig. 3 shows the in situ DRIFTS spectra of Ag/Al_2O_3
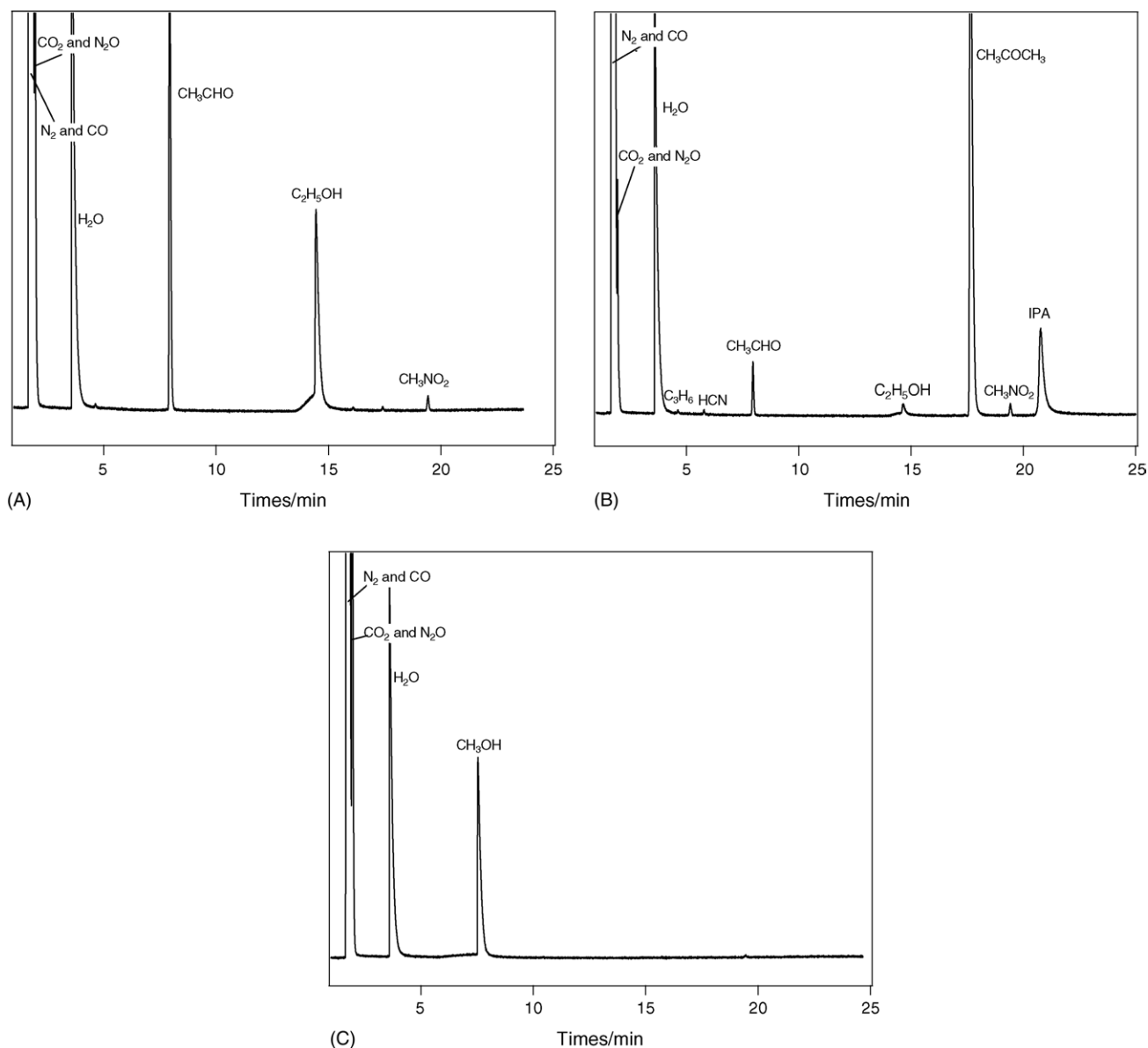
Fig. 2. (A) GC–MS chromatogram of gas products of $C_2H_5OH/NO/O_2$ reaction at 473 K on Ag/Al_2O_3 catalyst. Conditions: NO 800 ppm; C_2H_5OH 1565 ppm; O_2 10%. (B) GC–MS chromatogram of gas products of $IPA/NO/O_2$ reaction at 473 K on Ag/Al_2O_3 catalyst. Conditions: NO 800 ppm; IPA 1200 ppm; O_2 10%. (C) GC–MS chromatogram of gas products of $CH_3OH/NO/O_2$ reaction at 473 K on Ag/Al_2O_3 catalyst. Conditions: NO 800 ppm; CH_3OH 2250 ppm; O_2 10%.

catalyst in the flow of NO + C_2H_5OH + O_2 in steady state at various temperatures. Based on the previous study [19], the bands at 1633, 1416 and 1336 cm^{-1} are assignable to the enolic species and the peaks at 1578 and 1464 cm^{-1} are associated with acetate species, whereas the bands at 1585 and 1304 cm^{-1} are due to adsorbed nitrates. In addition, a very strong peak appeared at 2233 cm^{-1}, which is assignable to –NCO species. During NO + IPA + O_2 reaction over Ag/Al_2O_3 catalyst (Fig. 4), the characteristic peaks are similarly assigned to enolic species (1633, 1412 and 1338 cm^{-1}), acetate species (1579 and 1468 cm^{-1}) and nitrates (1585 and 1302 cm^{-1}). The shoulder peak at 1612 cm^{-1} was also assigned to bridge adsorbed surface nitrate species [7,15,19]. The obvious difference is the

appearance of the formate bands at 1591 and 1382 cm^{-1}, while the peak at 1392 cm^{-1} could be associated with δ(C–H) [13,17,19,22]. In the case of NO + CH_3OH + O_2 reaction (Fig. 5), very weak –NCO peak at 2233 cm^{-1} and strong formate peaks at 1595 and 1379 cm^{-1} were observed. Whereas the bands at 1300, 1589 and 1612 cm^{-1} are similarly assigned to adsorbed nitrates and the band at 1390 cm^{-1} is associated with δ(C–H), as shown in Fig. 4. The bands at 1639, 3732, 3697 and 3589 cm^{-1} are considered to relate with the formation of H_2O by dehydration of CH_3OH and it disappeared by increasing temperature to 623 K. According to the literature [20,21], CH_3OH was selectively dehydrated to dimethyl ether (DME) over γ-Al_2O_3 and promoted γ-Al_2O_3 in the
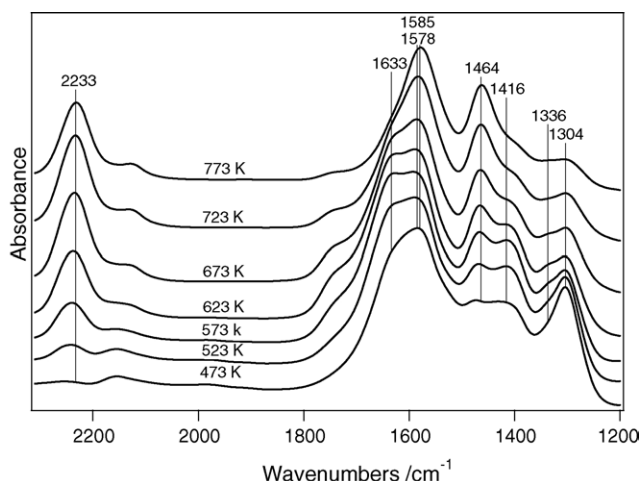
Fig. 3. In situ DRIFTS spectra of adsorbed species in steady state on Ag/Al$_2$O$_3$ in a flow of C$_2$H$_5$OH + O$_2$ + NO at various temperatures. Conditions: NO 800 ppm; C$_2$H$_5$OH 1565 ppm; O$_2$ 10%.

Fig. 5. In situ DRIFTS spectra of adsorbed species in steady state on Ag/Al$_2$O$_3$ in a flow of CH$_3$OH + O$_2$ + NO at various temperatures. Conditions: NO 800 ppm; CH$_3$OH 2250 ppm; O$_2$ 10%.

temperature of 423–573 K, accompanied by the formation of H$_2$O.

As shown in Figs. 3–5, the formation of –NCO species in the NO–O$_2$–C$_2$H$_5$OH is similar to that in the NO–O$_2$–IPA system, which is different from that in the NO–O$_2$–CH$_3$OH system. When the Ag/Al$_2$O$_3$ catalyst was exposed to a NO–O$_2$–CH$_3$OH mixture under the same experimental conditions, very weak band of –NCO species was observed compared with the cases using C$_2$H$_5$OH or IPA as reductants. We have proposed the mechanism of the SCR of NO$_x$ by C$_2$H$_5$OH over Ag/Al$_2$O$_3$, as shown in Scheme 1 [19]. It has been widely accepted that –NCO species is a crucial intermediate in the SCR of NO$_x$ over Ag/Al$_2$O$_3$ and its high productivity results in a high efficiency of NO$_x$ reduction. The linkage between the formation tendency of –NCO species and enolic species was clearly observed in Figs. 3–5. As for Ag/Al$_2$O$_3$, the order of the facility for the formation of –NCO species was in good agreement with the
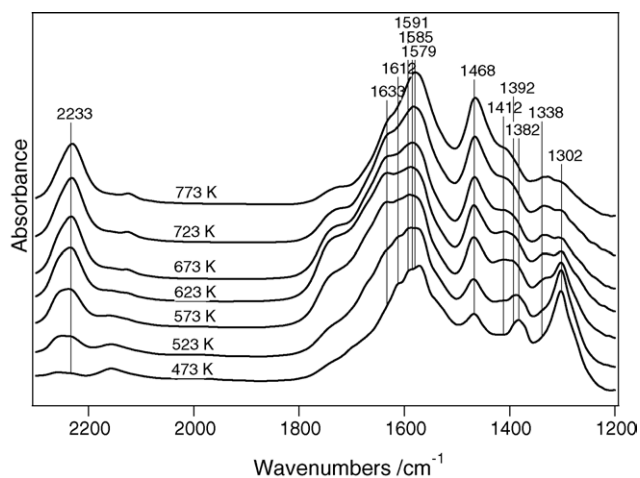
order of the activities in the SCR of NO$_x$ process (Fig. 1: C$_2$H$_5$OH > IPA > CH$_3$OH) in the moderate temperature range of 523–623 K.

GC–MS and FTIR experiments indicated the formation of nitrogen-containing molecule (such as CH$_3$NO$_2$) and oxygen-containing molecules (such as CH$_3$CHO and CH$_3$COCH$_3$) during the SCR of NO$_x$ by C$_2$H$_5$OH or IPA over Ag/Al$_2$O$_3$. Nitrogen-containing molecules and oxygen-containing molecules have been proposed to be the key intermediates in the reduction of NO$_x$ [3,4,15,19]. The analysis of gas products together with in situ DRIFTS spectra proved the similar mechanisms of the SCR of NO$_x$ by C$_2$H$_5$OH and IPA over Ag/Al$_2$O$_3$, whereas CH$_3$OH was not found to follow the similar mechanism. More evidences for the different reaction mechanisms will be discussed below.

3.3. Formation of adsorbed enolic species in the partial oxidation reaction over Ag/Al$_2$O$_3$

To elucidate the differences among the reductants for the SCR of NO$_x$ over Ag/Al$_2$O$_3$, we investigated the surface species formed on the Ag/Al$_2$O$_3$ catalyst during the oxidation reaction of different alcohols.

Fig. 6 shows the in situ DRIFTS spectra of Ag/Al$_2$O$_3$ at various temperatures in steady state after the exposure to

Fig. 4. In situ DRIFTS spectra of adsorbed species in steady state on Ag/Al$_2$O$_3$ in a flow of IPA + O$_2$ + NO at various temperatures. Conditions: NO 800 ppm; IPA 1200 ppm; O$_2$ 10%.
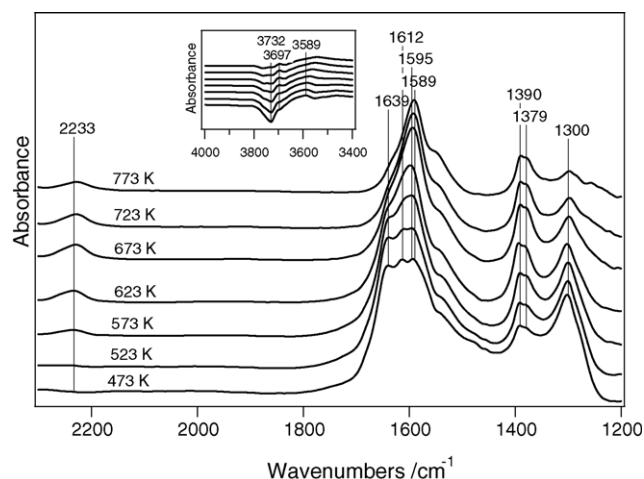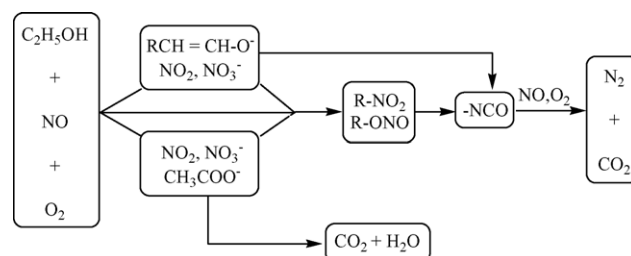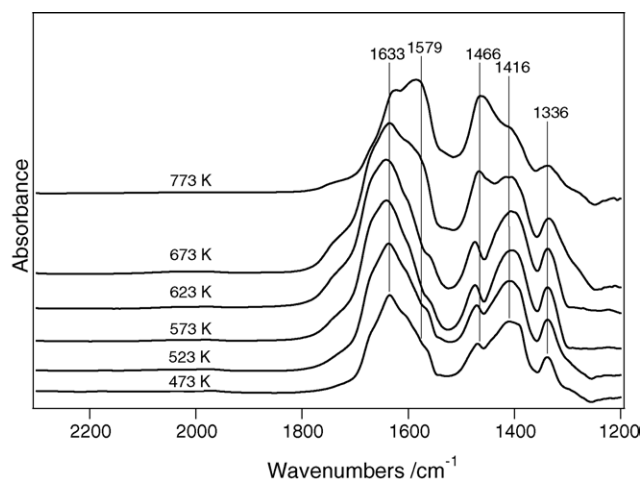

Scheme 1. The mechanism of the SCR of NO$_x$ by C$_2$H$_5$OH over Ag/Al$_2$O$_3$.

Fig. 6. In situ DRIFTS spectra of adsorbed species in steady state on Ag/Al$_2$O$_3$ in a flow of C$_2$H$_5$OH + O$_2$ at various temperatures. Conditions: C$_2$H$_5$OH 1565 ppm; O$_2$ 10%.

C$_2$H$_5$OH + O$_2$ mixture gas, where the five peaks appeared at 1633, 1416, 1336, 1579 and 1466 cm^{-1}. The peaks at 1633, 1416 and 1336 cm^{-1} are attributed to the enolic species and the peaks at 1579 and 1466 cm^{-1} are assigned to acetate species. As shown in Fig. 6, the enolic species is dominantly formed from the partial oxidation of C$_2$H$_5$OH in the temperature range of 473–673 K, whereas at 773 K, the enolic species was further oxidized into the acetate species.

The same set of experiment was conducted after exposing the catalyst to a flow of IPA + O$_2$. As shown in Fig. 7, within the temperature range of 573–723 K, a very strong peak at 1633 cm^{-1} due to the enolic species was also observed, which accompanied by the appearance of the peaks at 1408 and 1335 cm^{-1}. The bands at 1595 and 1379 cm^{-1} are assigned to formate species, the bands at 1581 and 1468 cm^{-1} are attributed to acetate species and the peak at 1392 cm^{-1} can be associated with δ(C–H), as the same as in Fig. 4. At low temperatures, the formate species was
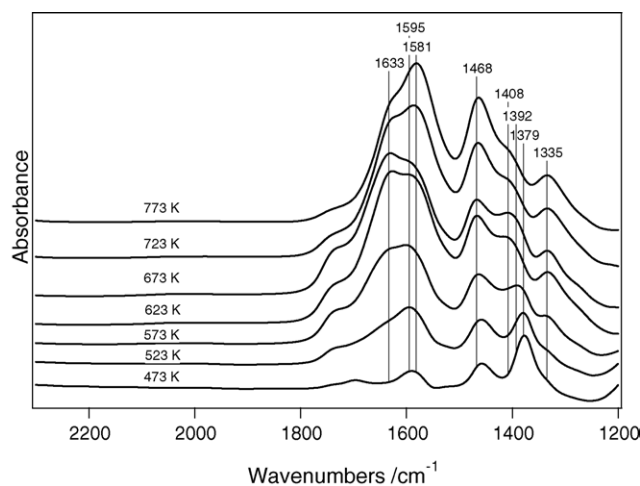

Fig. 7. In situ DRIFTS spectra of adsorbed species in steady state on Ag/Al$_2$O$_3$ in a flow of IPA + O$_2$ at various temperatures. Conditions: IPA 1200 ppm; O$_2$ 10%.
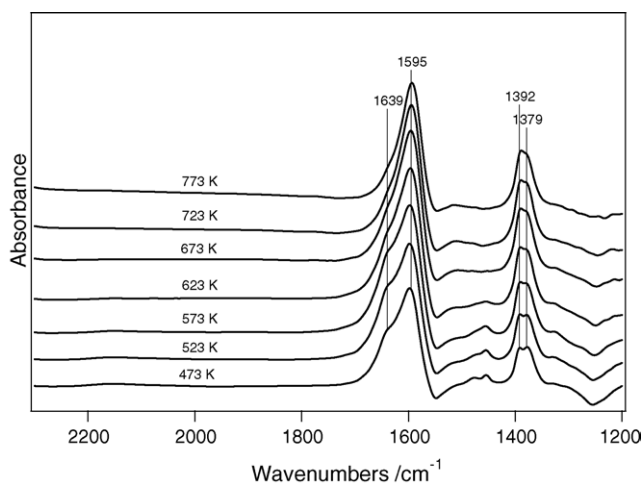

Fig. 8. In situ DRIFTS spectra of adsorbed species in steady state on Ag/Al$_2$O$_3$ in a flow of CH$_3$OH + O$_2$ at various temperatures. Conditions: CH$_3$OH 2250 ppm; O$_2$ 10%.

predominant, while within the temperature range of 623–673 K, the enolic species became predominant, indicating that the partial oxidation occurs preferentially on Ag/Al$_2$O$_3$. However, the acetate species resulted from further oxidation of the enolic species is dominant at temperatures above 723 K.

Exposing Ag/Al$_2$O$_3$ catalyst to a flow of CH$_3$OH + O$_2$ resulted in the appearance of four peaks (1639, 1595, 1392 and 1379 cm^{-1}). As can be seen from Fig. 8, the band at 1595 and 1379 cm^{-1} are assigned to the formate species and the very weak band at 1639 cm^{-1} is due to the formation of H$_2$O by dehydration of CH$_3$OH, as discussed in Fig. 5. While the peak at 1392 cm^{-1} is associated with δ(C–H). Apparently, the deep oxidation of CH$_3$OH occurred preferentially above 573 K on Ag/Al$_2$O$_3$, because the formate species is predominant during the oxidation reaction and the characteristic bands of the enolic species were not detected in this study. Comparative studies show that partial oxidation of CH$_3$OH is different from that of other alcohols. As a fact, while the enolic species was the dominant surface species on Ag/Al$_2$O$_3$ during the partial oxidation of C$_2$H$_5$OH and IPA, it is not the case for CH$_3$OH, which may account for the relatively low efficiency in the SCR of NO$_x$.

3.4. Reactivity of the surface enolic species over Ag/Al$_2$O$_3$

To obtain further information on the reactivity of the surface enolic species, the reactivity of the enolic species toward NO + O$_2$ was studied by the transient response of DRIFTS method.

Fig. 9A shows the dynamic changes of in situ DRIFTS spectra of the adsorbed species in a flow of NO + O$_2$ on Ag/Al$_2$O$_3$ at 673 K. The integrated areas of these peaks in Fig. 9A are displayed as a function of time in Fig. 9B. When the catalyst was exposed to C$_2$H$_5$OH + O$_2$ for 60 min, very strong enolic species peaks appeared at 1633, 1416 and
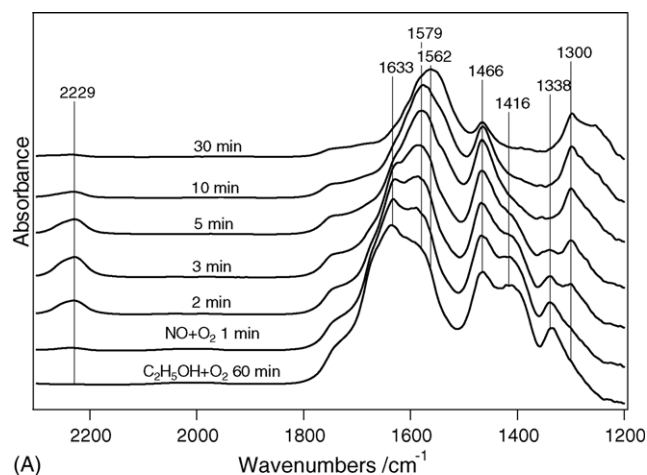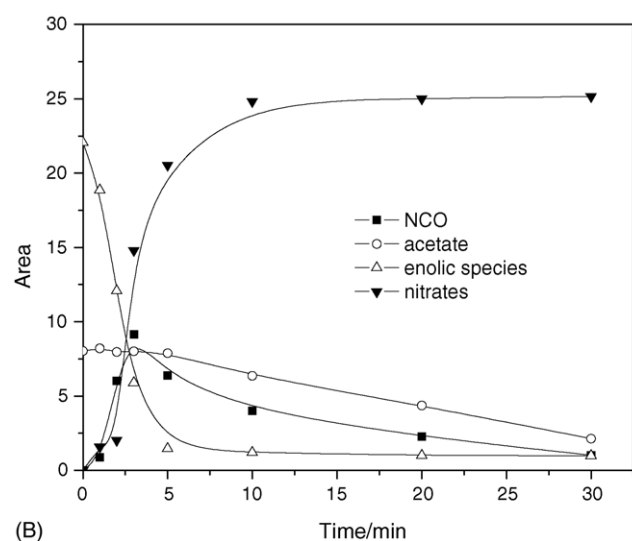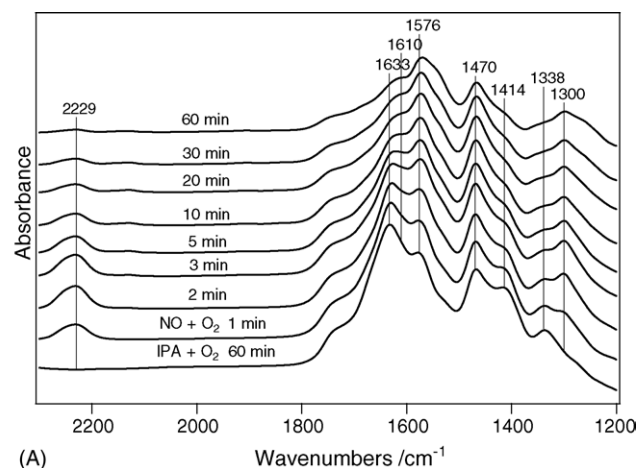
Fig. 9. (A) Dynamic changes of in situ DRIFTS spectra of adsorbed species on Ag/Al_2O_3 as a function of time in a flow of $NO + O_2$ at 673 K. Before measurement, the catalyst was pre-exposed to a flow of $C_2H_5OH + O_2$ for 60 min at 673 K. Conditions: NO 800 ppm; C_2H_5OH 1565 ppm; O_2 10%. (B) Time dependence of the integrated areas of the peaks for different adsorbed species in (A): (■) –NCO, 2160–2308 cm^{-1}; (○) acetate, 1440–1505 cm^{-1}; (▼) nitrates, 1210–1322 cm^{-1}; (△) enolic species 1612–1710 cm^{-1}).
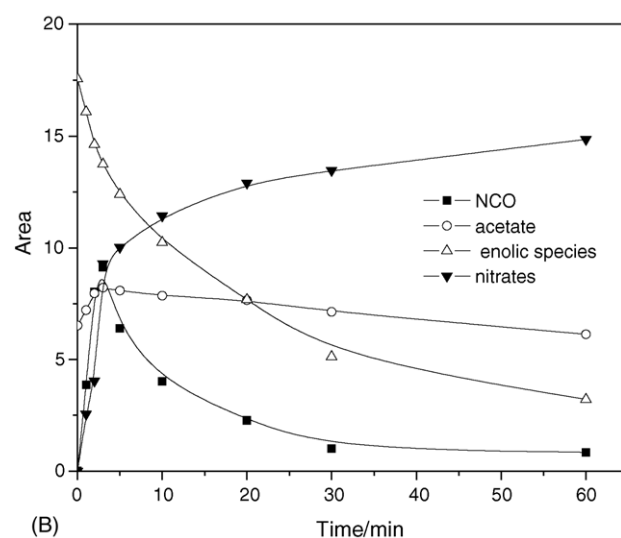

Fig. 10. (A) Dynamic changes of in situ DRIFTS spectra of adsorbed species on Ag/Al_2O_3 as a function of time in a flow of $NO + O_2$ at 673 K. Before measurement, the catalyst was pre-exposed to a flow of $IPA + O_2$ for 60 min at 673 K. Conditions: NO 800 ppm; IPA 1200 ppm; O_2 10%. (B) Time dependence of the integrated areas of the peaks for different adsorbed species in (A): (■) –NCO, 2160–2308 cm^{-1}; (○) acetate, 1440–1505 cm^{-1}; (▼) nitrates, 1210–1322 cm^{-1}; (△) enolic species, 1612–1710 cm^{-1}.

1338 cm^{-1} and acetate peaks were also observed at 1579 and 1466 cm^{-1}. Switching the feed gas to a flow of $NO + O_2$ resulted in a sharp decrease of the enolic species. Meanwhile, a new –NCO peak appeared at 2229 cm^{-1}, with its intensity increased initially and then decreased after it reached a maximum. The linkage between the formation of the –NCO species and the consumption of the enolic species strongly suggests the participation of the enolic species in the formation of –NCO species. When the enolic species was completely consumed, a large amount of nitrates and acetate became dominant surface species on Ag/Al_2O_3, while the surface concentration of –NCO was very low. This result indicates that the enolic species effectively reacts toward $NO + O_2$ to form –NCO species than acetate species does. As a result, it is the enolic species rather than the acetate

species, that plays a crucial role in the –NCO formation by reaction with $NO + O_2$.

The same experiment was performed after exposing the catalyst to a flow of $IPA + O_2$ and we derived the same conclusion. As shown in Fig. 10A and B, after switching the feed gas to $NO + O_2$ within 30 min, the intensity of the enolic species decreased, accompanied by a clear increase in the intensity of –NCO species. This result strongly confirms that the enolic species is the key intermediate in the formation of –NCO.

Fig. 11A shows the dynamic changes of in situ DRIFTS spectra of the Ag/Al_2O_3 catalyst firstly exposed to $CH_3OH + O_2$ for 60 min at 673 K and then switched to a flow of $NO + O_2$. Compared with C_2H_5OH and IPA, it should be noted that the peak due to the enolic species
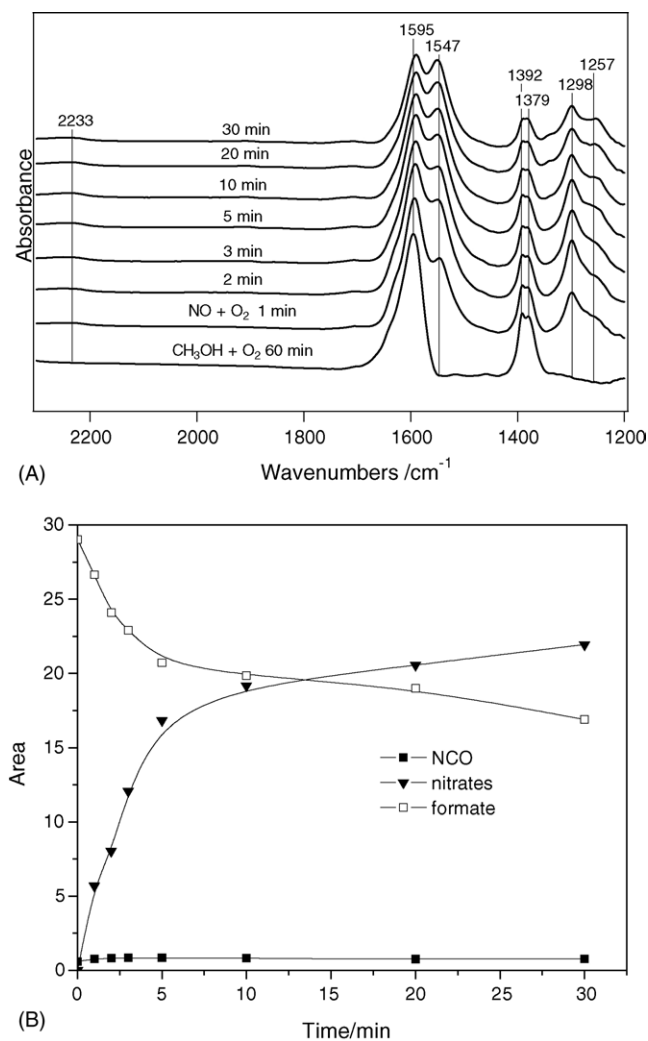
Fig. 11. (A) Dynamic changes of in situ DRIFTS spectra of adsorbed species on Ag/Al_2O_3 as a function of time in a flow of $NO + O_2$ at 673 K. Before measurement, the catalyst was pre-exposed to a flow of $CH_3OH + O_2$ for 60 min at 673 K. Conditions: NO 800 ppm; CH_3OH 2250 ppm; O_2 10%. (B) Time dependence of the integrated areas of the peaks for different adsorbed species in (A): (■) –NCO, 2160–2308 cm^{-1}; (▼) nitrates, 1210–1322 cm^{-1}; (□) formate, 1533–1720 cm^{-1}.

(around 1633 cm^{-1}) was not observed, whereas the peaks of the formate species (1595 and 1379 cm^{-1}) were very strong. On the other hand, very weak band due to the –NCO species (2233 cm^{-1}) was observed, as can be seen from Fig. 11A and B. This result strongly suggests again that the enolic species plays a crucial role in the –NCO formation during the SCR of NO_x by alcohols.

4. Conclusions

Based on the DRIFTS studies, the enolic species has been proved to be the main surface species during the partial oxidation of C_2H_5OH or IPA over Ag/Al_2O_3 catalyst. The high reactivity of the enolic species with $NO + O_2$ results in high surface concentration of –NCO species and high efficiency of NO_x reduction when using C_2H_5OH or IPA as reductants in the SCR of NO_x. The linkage between the formation of the –NCO species and the consumption of the enolic species has been found. We have confirmed the similar mechanisms of the SCR of NO_x by C_2H_5OH and IPA over Ag/Al_2O_3. However, CH_3OH has not been found to follow the similar mechanism. CH_3OH is much less reactive for the formation of –NCO species. The order of the facility for the formation of enolic species and –NCO species is in good agreement with the order of the activities ($C_2H_5OH > IPA > CH_3OH$) in the moderate temperature range of 523–623 K during the SCR of NO_x.

References

[1] T. Midyadera, Appl. Catal. B 2 (1993) 199.
[2] K.A. Bethke, H.H. Kung, J. Catal. 172 (1997) 93.
[3] S. Sumiya, H. He, A. Abe, N. Takezaka, K. Yoshida, J. Chem. Soc. Faraday Trans. 94 (1998) 2217.
[4] S. Sumiya, M. Saito, H. He, Q.-C. Feng, N. Takezawa, Catal. Lett. 50 (1998) 87.
[5] A. Abe, N. Aoyama, S. Sumiya, N. Kakuta, K. Yoshida, Catal. Lett. 51 (1998) 5.
[6] F.C. Meunier, V. Zuzaniuk, J.P. Breen, M. Olsson, J.R.H. Ross, Catal. Today 59 (2000) 287.
[7] K. Shimizu, J. Shibata, H. Yoshida, A. Satsuma, T. Hattori, Appl. Catal. B 30 (2001) 151.
[8] F.C. Meunier, R. Ukropec, C. Stapleton, J.P. Breen, Appl. Catal. B 30 (2001) 163.
[9] R. Burch, J.P. Breen, F.C. Meunier, Appl. Catal. B 39 (2002) 283.
[10] E.F. Iliopoulou, A.P. Evdou, A.A. Lemonidou, I.A. Vasalos, Appl. Catal. A 274 (2004) 179.
[11] Y. Ukisu, S. Sato, A. Abe, K. Yoshida, Appl. Catal. B 2 (1993) 147.
[12] Y. Ukisu, T. Miyadera, A. Abe, K. Yoshida, Catal. Lett. 39 (1996) 265.
[13] T. Chafik, S. Kameoka, Y. Ukisu, T. Miyadera, J. Mol. Catal. A 136 (1998) 203.
[14] F.C. Meunier, J.P. Breen, V. Zuzaniuk, M. Olsson, J.R.H. Ross, J. Catal. 187 (1999) 493.
[15] S. Kameoka, Y. Ukisu, T. Miyadera, Phys. Chem. Chem. Phys. 2 (2000) 367.
[16] N. Bogdanchikova, F.C. Meunier, M. Avalos-Borja, J.P. Breen, A. Pestryakov, Appl. Catal. B 36 (2002) 287.
[17] N. Bion, J. Saussey, M. Haneda, M. Daturi, J. Catal. 217 (2003) 47.
[18] A. Satuma, K. Shimizu, Prog. Energy Combust. Sci. 29 (2003) 71.
[19] Y. Yu, H. He, Q. Feng, H. Gao, X. Yang, Appl. Catal. B 49 (2004) 159.
[20] S.G. Masters, D. Chadwick, Catal. Today 42 (1998) 137.
[21] S.G. Masters, D. Chadwick, Appl. Catal. B 23 (1999) 235.
[22] Standard IR Spectra, Sadtler Research Labs.